Electronic and chemical properties of In and Sb adsorbed on Ge(100) studied by synchrotron photoemission

D. H. Rich,* T. Miller, and T.-C. Chiang
Department of Physics, University of Illinois at Urbana-Champaign, 1110 West Green Street, Urbana, Illinois 61801 and Materials Research Laboratory, University of Illinois at Urbana-Champaign, 104 South Goodwin Avenue, Urbana, Illinois 61801
(Received 17 July 1989)

The initial stages of interface formation for In and Sb, each separately adsorbed on the Ge(100)-(2×1) surface, have been investigated for various submonolayer coverages with use of synchrotron-photoemission and high-energy electron-diffraction techniques. By examining the evolution of the substrate and adsorbate core-level line shapes during the adsorbate growth it is possible to deduce chemical and structural information. The dimer-related surface-shifted component of the Ge 3*d* core level is found to gradually convert into a component possessing a binding energy indistinguishable from the bulk component for increasing Sb coverages. For submonolayer In depositions, this surface-shifted component results in a chemically shifted interface component which is distinguishable from the emission from bulk atoms and unreacted Ge dimers. The resulting chemical shifts are consistent with expectations based on electronegativity arguments. For both In and Sb, the adsorbate-to-substrate bonding coordination number is obtained for various submonolayer coverages. The homogeneity of the adsorbate bonding is evaluated by examining the width of the In and Sb 4*d* core-level line shapes. The Fermi-level position relative to the gap for various In and Sb coverages and the Schottky-barrier heights are obtained. Photoemission from the valence bands shows a modification in the dimer-derived surface states upon In and Sb adsorption; the surfaces show little density of states at the Fermi level for coverages below 1 monolayer. Structural models for the In/Ge(100)-(2×2) and Sb/Ge(100)-(2×1) surfaces which correlate with the data are discussed.

I. INTRODUCTION

The adsorption and growth of III-V compounds on the Si and Ge surfaces have attracted much attention in recent years. The relatively mature Si-based microelectronics industry should serve as an ideal foundation for the future fabrication of III-V integrated-circuit components relying on single-heterostructure, superlattice, and quantum-well forms of construction on Si and Ge substrates. Basic device performance largely depends on the ability to produce high-quality epitaxial growth of III-V films on the substrate. In order to optimize the material properties, it is essential that basic information concerning the interface, such as atomic and electronic structure and the barrier height, be well known. Although much emphasis has been placed on the GaAs/Si interface, it is important to investigate the behavior of various $A^{III}B^{V}/C^{IV}$ systems for a better understanding of the effects of lattice mismatch, surface reconstruction, surface-step morphology, electronic interface-barrier formation, and the basic adsorbate-to-substrate interface chemistry.

This work is a study of the initial stages of interface formation of In and Sb, each separately, with the Ge(100) surface with use of the techniques of synchrotron-photoemission spectroscopy and high-energy electron diffraction (HEED). The HEED measurements are used to determine changes in the long-range periodicity and assess the overall quality of the adsorbate-induced reconstructions on Ge(100). Basic electronic and chemical characteristics of each interface formation are evaluated by assessing changes occurring in the Ge 3*d*, Sb 4*d*, and In 4*d* core-level line shapes and binding energies during the submonolayer growth. The In/Ge(100) data are compared with previous photoemission and HEED results for In/Si(100).[1] Like Si(100)-(2×1), the Ge(100)-(2×1) surface is known to consist of dimers which contain one dangling bond per surface atom; the dimer nature on both surfaces has been confirmed by scanning tunneling microscopy (STM).[2,3] The dimers give rise to a distinct shift relative to the bulk in the core-level line shape. The photoemission intensity from the surface-shifted component is a direct measure of the number of dimer dangling bonds on the surface. With adsorbate coverage on the surface, some of the dangling bonds may become involved in the chemisorption bonding, and the core-level binding energies of the corresponding surface atoms may change. By examining the modification of the substrate core-level line shape, it is possible to determine the average number of surface dangling bonds which are modified in the presence of an adatom for various submonolayer coverages; this quantity is just the adsorbate-to-substrate bonding coordination number (BCN).[1] The BCN is a quantity of fundamental interest in surface studies, since it provides important information concerning the chemistry of surface dangling bonds and the resulting adsorption geometry. The determination of the BCN using the core-level photoemission technique was first demonstrat-

ed for In/Si(100),[1] and later performed for Sn,[4] Ag,[5] and Sb (Ref. 6) deposited on Si(100). For these systems, the BCN, adsorbate core-level, valence-band, and electron-diffraction measurements have led to structural models which correlate well with the data.[1,4,5] In this paper we show that this approach may be extended to other substrates which possess a well-defined surface core-level shift, such as Ge(100)-(2×1).

The Ge 3*d* core-level line shape of clean Ge(100)-(2×1) has been investigated in some detail.[7–10] The intensity of the surface-shifted component of a core level reflects the relative population of the surface sites, and a precision quantification of this relation is essential for adsorption studies. A previous investigation of Cl adsorption on Ge(100) has sought to quantify the surface-shifted component by comparing the intensity of the chemically shifted component with the clean-surface intensity; the contribution of Ge surface atoms to the shifted core level was reported to be about 0.62 monolayer (ML).[9] In another previous study, a reference surface consisting of a known submonolayer coverage of Ge deposited on Si(100) was used to perform an *in situ* comparison with the Ge(100)-(2×1) surface, and 0.87 ML of Ge surface atoms were found to contribute to the surface component.[10] The present study will further examine the relationship between the clean-surface emission and the resulting emission from adsorbate-bonded Ge interface atoms.

The Sb 4*d* and In 4*d* core-level line shapes were examined to evaluate the relative homogeneity of the adsorbate site bonding. For a given adsorbate, sites which possess distinctly different local chemical environment due to variations in bond hybridization and coordination number may show distinct binding-energy shifts.[11] Furthermore, an evaluation of changes in binding energy relative to the valence-band maximum (VBM) during the adsorbate growth can indicate the degree to which the adsorbate has been incorporated into the local bulk-crystal electrostatic potential.[4] The intensity variation of both adsorbate and substrate core levels is also crucial in evaluating the natures of the overlayer growth mode, sticking coefficient, bulk diffusion, and surface segregation.

Changes in electronic properties are further evaluated by examining the valence-band density of states near the Fermi level. Changes in surface states and formation of interface states may occur during the overlayer growth, and correlations between surface core-level emission and surface states during overlayer growth has been previously investigated for a variety of systems.[12] The Fermi-level position relative to the gap has been measured as a function of adsorbate coverage, and the Schottky-barrier heights are obtained.

II. EXPERIMENTAL DETAILS

The photoemission experiments were carried out with use of synchrotron radiation from the University of Illinois beam line on Aladdin, the 1-GeV storage ring at the Synchrotron Radiation Center of the University of Wisconisn–Madison at Stoughton, Wisconsin. Light from the ring was dispersed by an "Extended Range Grasshopper" monochromator, which was designed and constructed by Brown and his co-workers.[13] The photoelectrons were analyzed with a Leybold-Heraeus EA-10 hemispherical electrostatic analyzer. The overall instrumental resolution was about 0.2 eV. The sample Fermi level was determined by observing emission from the Fermi edge of a polycrystalline Au sample in electrical contact with the Ge samples.

The *p*-type Ge(100) sample was aligned by Laue diffraction to within 1° and mechanically polished to a mirror finish. The clean Ge(100) surface was prepared by repeated cycles of argon-ion sputtering at 400 °C and further annealing at 600 °C after sputtering. A small mixture of quarter-order and half-order spots indicative of some $c(4\times2)$ and (2×2) ordering was observed within a sharp two-domain (2×1) pattern. It is the intensity of the (2×1) pattern which suggests the nominal Ge(100)-(2×1) convention used here. The In and Sb overlayers on Ge(100) were prepared by evaporation from electron-beam-heated crucibles each containing 99.999% pure elemental In and Sb. The rate of deposition was separately monitored for each material using a quartz crystal thickness monitor and was maintained at about 1 ML/min. In this paper 1 ML of In or Sb is defined as 6.24×10^{14} atoms/cm^2 which is the site-number density for the unreconstructed Ge(100) surface.

III. RESULTS FOR Sb/Ge(100)

A. Coverage versus exposure

Two substrate temperatures, $T=50$ and 400 °C, were used in the growth of Sb on Ge. At the lower growth temperature, the Sb vapor simply condenses on the substrate. Thus, the measured exposure equals the coverage. At the higher temperature, the buildup of Sb on the substrate stops after ~1 ML exposure due to saturation of all bonding sites and reevaporation; this behavior is simi-

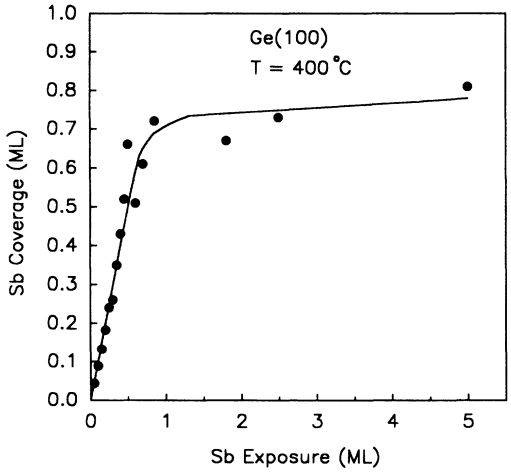

FIG. 1. The Sb coverage as a function of the Sb exposure on Ge(100) with the substrate temperature maintained at 400 °C during exposure. A solid line is shown through the data to serve as a guide for the eye.

lar to that of the Sb/Si(100) system.[6,14,15] Therefore, it becomes necessary to distinguish the exposure from the coverage. Also, the bulk solubility of Sb in Ge is ~0.01% at 600 °C;[16] thus Sb incorporation into bulk Ge is not expected to be significant under our experimental conditions. By comparing the Sb core-level intensities from samples prepared at these two temperatures, it is possible to deduce the coverage from the exposure for the high-temperature case. For Sb exposures less than ~0.5 ML, the Sb coverages are found to be equal to the Sb exposures. The results are summarized in Fig. 1. The smooth curve is a guide to the eye, which shows a saturation behavior.

B. HEED

For growth at $T=50$ °C, the as-deposited Sb gradually diminished the intensity of the $\frac{1}{2}$-order lines of the original (2×1) pattern. The $\frac{1}{2}$-order line intensities are significantly reduced at 0.5 ML coverage relative to the primary, and further deposition of Sb results in a (1×1) diffuse pattern at 1 ML coverage. This suggests that as-deposited Sb on Ge(100) at near room temperatures is disordered. For $T=400$ °C, the (2×1) pattern is seen to remain for all Sb exposures in this study. The quality of the (2×1) pattern is seen to gradually diminish with the lines becoming more diffuse as the coverage approached saturation.

C. Ge 3*d* core level

The Ge 3*d* core-level line shape for clean Ge(100)-(2×1) has been previously analyzed.[7,10] As with the case of Si(100)-(2×1), a distinct surface shift is found toward lower binding energies. The experimental result (dots), the overall fit (solid line), and the surface and bulk contributions (labeled *B* and *S*, offset in the vertical direction for clarity) for a photon energy of 90 eV are shown at the bottom of Fig. 2. In short, the fit involves a bulk and a surface-shifted component, each represented by a spin-orbit split doublet, riding on a cubic polynomial background. The doublet is represented by the sum of two Voigt functions (convolution of a Gaussian with a Lorentzian). The background function, surface shift, spin-orbit splitting, $I(d_{5/2})/I(d_{3/2})$ intensity ratio (branching ratio), Lorentzian width, Gaussian width, and the surface and bulk emission intensities are treated as fitting parameters. The relative binding-energy scale in Fig. 2 is referred to the bulk contribution of the Ge $3d_{5/2}$ core level which is at 29.32 eV below the VBM.[7] This energy is an intrinsic property of the Ge crystal and is independent of the adsorbate coverage. The surface core-level shift is −0.43 eV from the fit, and other relevant parameters can be found in previous publications.[7,10]

The results for the Sb-covered surfaces are also shown in Fig. 2 for $T=400$ °C. The line shapes indicate that the surface-shifted component in the clean case is simply reduced by the Sb coverage, implying that the surface atoms after bonding to Sb assume a bulklike binding energy. Thus, the spectra were analyzed in the same manner as in the clean case. The surface shift was left as a variable in the fits to test the accuracy of the model, and the results indeed indicate that the surface shift remains close to −0.43 eV for all Sb coverages. The highest exposure which shows a barely detectable surface-shifted component is about 0.6 ML, and after which any further Sb exposure is not found to induce any measurable changes in the line shape. The conversion of the surface core-level binding energy to a bulklike value by Sb adsorption observed here is similar to that reported before for In, Sn, Ag, and Sb adsorption on Si(100).[1,4–6] The Ge 3*d* core-level line shapes for $T=50$ °C show a very similar behavior and therefore not shown here. The *S*-component weight (the intensity of the shifted component relative to the total intensity) is shown in Fig. 3 as a function of Sb exposure. The results are indeed very similar for both growth temperatures.

From the measured *S*-component weight, the number

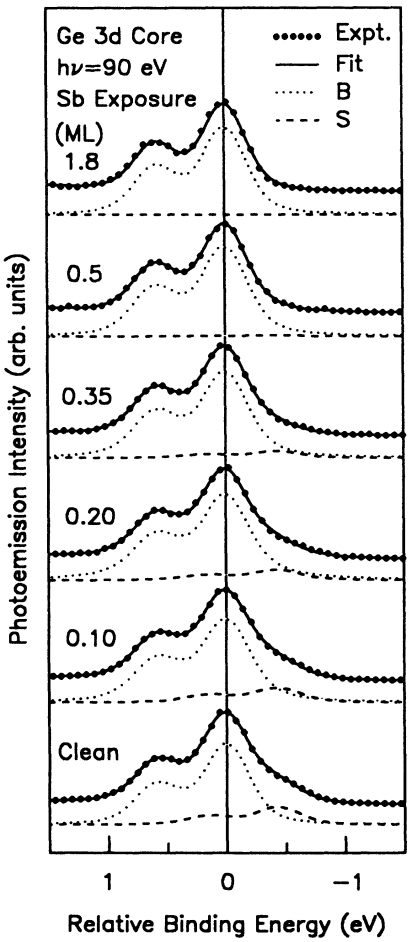

FIG. 2. Ge 3*d* core-level spectra (dots) taken with a photon energy of 90 eV for the clean Ge(100)-(2×1) surface and Sb-covered Ge(100) prepared at growth temperature $T=400$ °C. The Sb exposures are indicated. The solid curves are the result of a fit to the data. The decomposition of the spectra into bulk (*B*) and surface (*S*) contributions are shown by the dotted and dashed curves, respectively. The relative binding energy scale is referred to the Ge $3d_{5/2}$ core-level component of the bulk contribution.

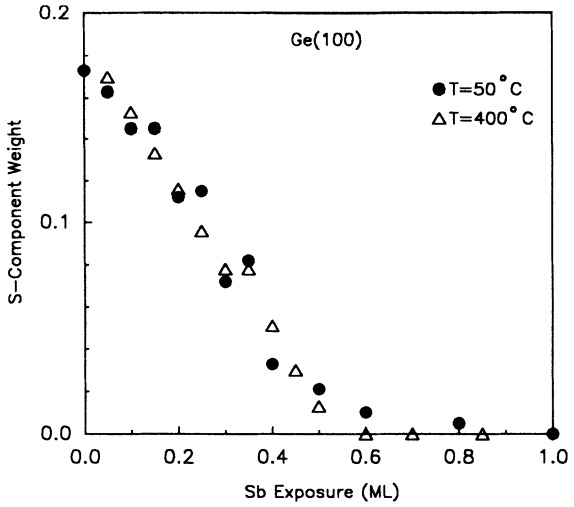

FIG. 3. The S-component weight (fraction of total intensity) for various Sb exposures on Ge(100). Solid circles and open triangles indicate data for growth temperatures $T=50$ and 400 °C, respectively.

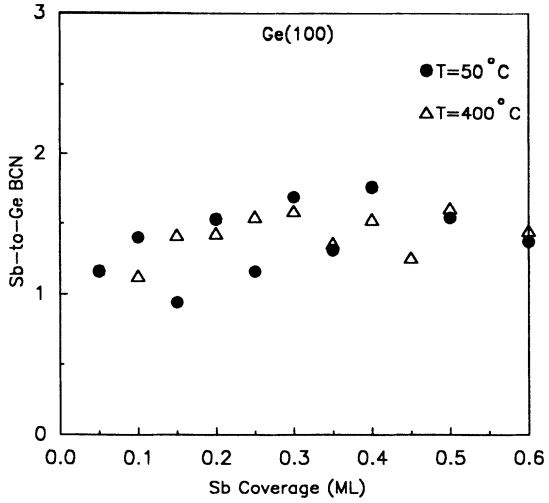

FIG. 4. The Sb-to-Ge bonding coordination number (BCN) for various Sb coverages on Ge(100). Solid circles and open triangles indicate data for growth temperature $T=50$ and 400 °C, respectively.

of Ge monolayers contributing to the shifted core-level component for various Sb coverages can be obtained. The clean-surface contribution to the S-component emission has previously been determined to be 0.87 ± 0.09 ML.[10] It was further concluded in this study that both kinds of dimers, buckled and nonbuckled, contribute to the S-component emission, and the departure from the ideal case (1 ML) was attributed to missing-dimer-type defects. Although another previous study yielded a different value (0.62 ML) for the surface-shifted contribution,[9] we believe that the 0.87 ML value is a more accurate one, and this value will be used below for the analysis. A detailed discussion of this point will be given later.

The reduction in intensity of the surface-shifted component for increasing Sb coverages is directly related to the number of surface dangling bonds being saturated by Sb adsorption. These atoms, after bonding to the Sb, exhibit a bulklike binding energy. From the results in Fig. 3, the average number of Ge surface atoms bonded to each Sb adatom (the BCN) is obtained and shown in Fig. 4.[1,4–6] The data extend to 0.6 ML Sb coverage only, because essentially all dangling bonds are saturated beyond this coverage and no surface-shifted component remains in the spectra. The uncertainty in the Ge dimer-atom population on the clean surface leads to a systematic error of about 10% in the data points shown in Fig. 4; random fluctuations are due to the limited experimental precision. The BCN for both substrate temperatures is initially about 1 for Sb coverages below 0.1 ML and increases to about 1.5 at 0.4 ML, and then decreases slightly to about 1.4 before and disappearance of the S component at ~0.6 ML. These data suggest that the initial interaction of Sb with Ge(100) is relatively insensitive to the substrate temperatures tested here.

The bulk Ge $3d$ core-level binding energy is found to change with respect to the measured Fermi-level position as a function of Sb exposure. This band-bending shift does not show in Fig. 2 because the spectra are aligned with respect to the VBM (with a constant offset). The clean Ge(100)-(2×1) surface is known to be p type, with the Fermi-level position residing about 0.1 eV above the VBM.[17] Figure 5 shows the Fermi-level position relative to the VBM (the energy zero) as a function of Sb exposure. The results are very similar for the two growth temperatures at exposures below ~0.7 ML. This is consistent with the earlier suggestion that the initial Sb-Ge

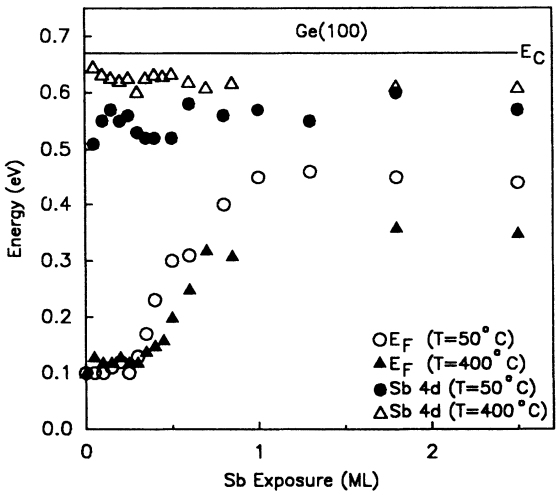

FIG. 5. The Fermi-level positions (open circles and solid triangles for growth temperatures $T=50$ and 400 °C, respectively) and the Sb $4d_{5/2}$ core-level binding energies (solid circles and open triangles for $T=50$ and 400 °C, respectively) for various Sb exposures. The Sb $4d_{5/2}$ binding energies have been offset 32.47 eV relative to the valence-band maximum (energy zero) to illustrate the correlations with the band edges. E_C denotes the conduction-band minimum of Ge.

interaction is similar for the two growth temperatures (see Fig. 3 and related discussion). At higher exposures, the resulting Schottky-barrier height is found to be 0.45±0.05 eV for $T=50$ °C and 0.35±0.05 eV for $T=400$ °C. The difference here is probably mainly related to the amount of Sb on the surface; the Sb coverage on the substrate at $T=400$ °C saturates at ~0.7 ML, while the buildup of Sb on the substrate at $T=50$ °C is continuous.

D. Sb 4*d* core level

The Sb 4*d* core-level spectra (dots for both growth temperatures are shown in Fig. 6 for various exposures. The spectra were fit with a spin-orbit-split doublet riding on a cubic polynomial background. The spin-orbit splitting and branching ratio are found to be coverage and temperature independent from the fit within tight tolerances, and the statistical averages are 1.246±0.008 eV and 0.703±0.013, respectively. The Lorentzian width for all exposures was constrained to 0.266 eV in the fitting procedure, which was the value obtained from the lowest exposure.

The Sb 4*d* Gaussian full width at half maximum (FWHM) from the fit is shown in Fig. 7 for both growth temperatures, which provides a measure of the homogeneity of the Sb site bonding. For example, Sb bonded to Sb and Sb bonded to Ge may not exhibit exactly the same core-level binding energy. Second nearest-neighbor effects can also lead to small shifts.[11] The effect of these unresolved small shifts on the line shape can be modeled by a Gaussian broadening. For $T=50$ °C, the Gaussian FWHM is seen to increase for exposures approaching 0.5 ML, and then to decrease for increasing exposures. For $T=400$ °C, the Gaussian FWHM is found to decrease for exposures approaching 0.5 ML, and then to level off. The data suggest that the sample prepared at the higher growth temperature has a greater degree of homogeneity. This is consistent with the HEED results, which show that the sample prepared at $T=50$ °C is disordered.

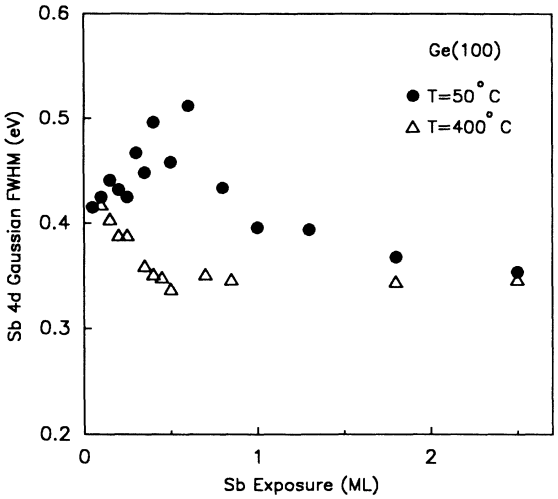

FIG. 7. The Sb 4*d* Gaussian full width at half maximum (FWHM) for various Sb exposures to Ge(100). Solid circles and open triangles indicate data for growth temperatures $T=50$ and 400 °C, respectively.

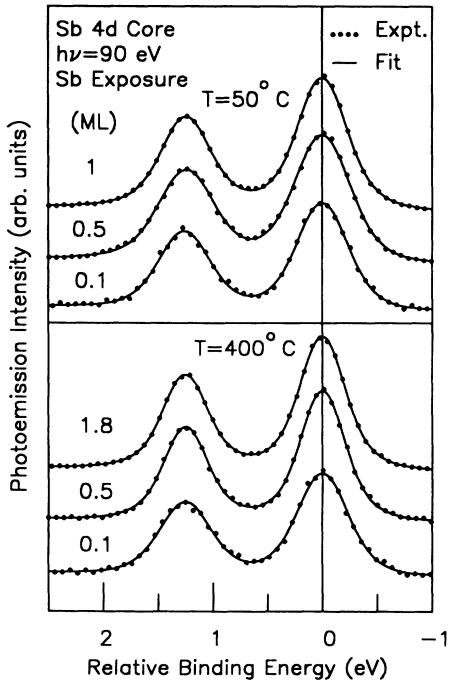

FIG. 6. The Sb 4*d* core-level spectra (dots) taken with a photon energy of 90 eV. The Sb exposures are indicated. The overall fits to the data are indicated by the solid curves. The upper and lower panels of the figure show the spectra taken for growth temperatures $T=50$ and 400 °C, respectively. The binding-energy scale is referred to the Sb $4d_{5/2}$ core-level component.

It is also interesting to examine the behavior of the Sb 4*d* core-level binding energy with respect to the band edges in order to assess the spatial extent of the crystal-potential barrier.[4] If a foreign atom is incorporated into the Ge lattice, its local electrostatic potential should be determined by the crystal, and its core-level binding energy should be tied to the VBM position. The results are shown in Fig. 5. The core-level data are shown in the figure with an arbitrary offset of 32.47 eV from its actual position to facilitate a comparison with the Fermi-level position and the band edges. For both growth temperatures, the Sb 4*d* core-level binding energy remains approximately constant relative to the band edges, while the Fermi-level position shows large changes. This suggests that the Sb cores are located within the dipole layer on the surface. Also, the Sb 4*d* core-level binding energies for the two growth temperatures are slightly different.

E. Valence bands

The valence-band photoemission spectra for various coverages, taken with a photon energy of 130 eV, are shown in Fig. 8. The clean Ge(100)-(2×1) spectrum is shown at the bottom of the figure. The binding energy is referenced with respect to the Fermi level labeled E_F in

the figure. These spectra should represent the density of states (DOS) to a good approximation in our angle-integrated geometry. The clean-surface spectrum shows a distinct hump, labeled *D* in the figure, situated about 1.2 eV below the Fermi level. Previous photoemission and STM experiments have investigated the possibility of a surface state on Ge(100)-(2×1). Rowe and Christman,[18] using an angle-integrated geometry and gas-exposure techniques, concluded that a peak located 1.3 eV below the Fermi level is derived from a dangling-bond-type surface state. Nelson *et al.*,[19] using angle-resolved photoemission in a normal-emission geometry, showed two states at 0.6 and 1.3 eV below the VBM which were sensitive to contamination and showed no dispersion with respect to the photon energy, and concluded these were derived from surface states. More recently, Hsieh *et al.* demonstrated with the "$k_\perp$ scan" technique that there is a significant bulk valence-band contribution to the 1.3-eV peak for photon energies less than ~16 eV.[20] For photon energies ranging from 24–45 eV Hsieh *et al.* showed that peaks located 0.5 and 1.3 eV below the Fermi level were nondispersive and could be due to surface-state emission. However, it was also pointed out that contributions from bulk critical points could not be ruled out. Kubby *et al.*,[2] using STM and tunneling spectroscopy, showed that a sharp surface-state peak derived from the Ge-dimer dangling bonds was located at 1.0 eV below the Fermi level. Differences in binding energy between the STM, angle-integrated, and angle-resolved photoemission experiments may be due to the varying degrees in which each technique samples $k_\parallel$. Thus, it is likely that the peak observed 1.2 eV below the Fermi level in Fig. 8 is due, at least in part, to surface-state emission; we adopt this interpretation here.

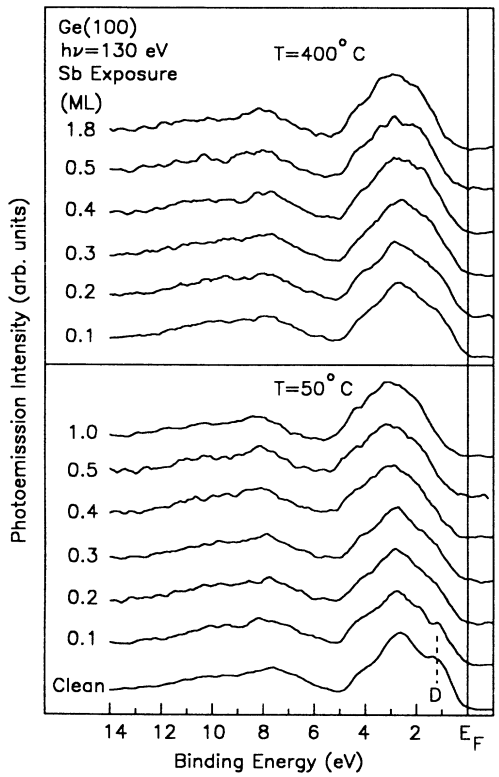

FIG. 8. The angle-integrated valence-band spectra taken with a 130 eV photon energy and shown for various Sb exposures on Ge(100). The upper and lower panels of the figure were for growth temperatures $T=400$ and 50 °C, respectively. The binding energy is referred to the Fermi level (E_F). The dashed line (labeled *D*) at 1.2 eV binding energy represents the position of the dimer dangling-bond surface state.

The surface-state feature for both growth temperatures is seen to be suppressed by the Sb adsorption. The peak becomes smeared into a shoulder for Sb coverages between 0.2 and 0.3 ML. Due to the overlapping intense bulk emission, it is impossible to quantify the reduction of the surface state, but the general trend is consistent with the Ge core-level data (Fig. 2) which showed that the surface core-level emission became suppressed through the saturation of the dangling bonds. A similar effect for various adsorbates on the Si(100)-(2×1) surface has been reported before.[1,4–6] In Fig. 8, the structures located 2–10 eV below the Fermi level are mainly derived from the bulk valence bands.[19,20] By overlaying these spectra, it is evident that there is a uniform movement of these features towards higher binding energies for increasing Sb coverages; this is due to the band bending discussed above (Fig. 5). At all exposures less than ~1 ML the density of states at the Fermi level remains low.

IV. RESULTS FOR In/Ge(100)

A. HEED

The In deposition was performed at a substrate temperature of 50 °C, which is much lower than the thermal desorption temperature of In. The bulk solubility of In in Ge is ~0.001% at 150 °C,[16] so In incorporation into the bulk should be negligible. Thus, the coverage equals the exposure. For In coverages below 0.2 ML, the HEED pattern remained similar to the original clean-surface (2×1) pattern. At approximately 0.2 ML additional weak $(\frac{1}{2},\frac{1}{2})$ diffraction lines were observed, indicating the formation of a (2×2) structure. The (2×2) structure became fully developed at 0.5 ML coverage, where the intensity of the primary and all $\frac{1}{2}$-order spots were about equal. For coverages greater than 0.5 ML, the (2×2) pattern is seen to diminish while a (4×1) pattern was observed to form for coverages between 0.5 and 1 ML. The $\frac{1}{4}$-order spots were seen to maximize in intensity at ~0.8 ML, and were less intense than the $\frac{1}{2}$-order spots in this coverage range. For coverages greater than 1 ML, a diffuse (1×1) pattern with a significant intensity modulation along the primary diffraction streaks was seen; this indicates the beginning of three-dimensional growth. When the 1-ML-covered Ge(100) surface was annealed for 1 min at 400 °C, a sharp (5×4) pattern was observed. The behavior at $T=50$ °C is similar to that of In/Si(100), which also showed an In-induced (2×2) pattern at 0.5 ML, followed by a three-dimensional growth for higher coverages.[1,21]

B. Ge 3*d* core level

The Ge 3*d* core-level spectra for the clean and In-covered surfaces are presented in Fig. 9. The deconvolution of the clean-surface spectrum into bulk and surface contributions has been discussed above (see Fig. 2). The surface-shifted component for the clean surface is seen to be gradually replaced by a hump with a binding energy in between the bulk and clean-surface contributions for increasing In coverages. As a first trial, a two-component analysis similar to the one used for Sb adsorption on Ge(100) was employed. The resulting intensity of the *S* component (the shifted component) was found to increase, and the shift of the *S* component was found to gradually move from the clean surface position of -0.43 to -0.33 eV for coverages approaching 0.5 ML. After ~ 0.5 ML coverage, the intensity of the *S* component stopped growing, and the binding energy remained fixed at -0.33 eV. Clearly, in this preliminary analysis, the movement of the *S* component relative to the *B* component is a result of emission from both reacted and unreacted dimers. Since no *S* component binding-energy shift is observed for coverages beyond ~ 0.5 ML, it is apparent that all Ge dimer atoms are reacted at this coverage and the chemically bonded In-to-Ge interface layer is fully developed. This correlates well with the full development of the (2×2) HEED pattern at this coverage. Therefore, a refinement of this fitting procedure is necessary to account for the differences between the reacted and unreacted portions of the surface. A third component labeled *C* has been introduced to account for emission from reacted Ge dimers in addition to the original *S* component which represents emission from unreacted dimers. During the fit, the relative binding energies of the *S* and *C* components were constrained to -0.43 and -0.33 eV, respectively, since these values reflect the binding energy of each type of site for the clean and fully reacted surfaces. The results of the fits are shown in Fig. 9. Since the *C* and *S* components have very similar shifts, it is important to assess the quality of the fit. The residue (difference between the data and fit) normalized to the peak height is shown in Fig. 10 for each of the six spectra in Fig. 9. The residue shows just noise and is seen to be less than 3% (the root-mean-square residue is about 1%); thus, the quality of the fits is high. The weights of the *S* and *C* components are plotted in Fig. 11 for various In coverages. The *S* component is seen to decrease linearly and disappear at 0.4–0.5 ML while the *C* component increases linearly and maximizes at the same coverage. If the behavior of the *C* component is ignored, the BCN can be obtained by analyzing the intensity reduction of the *S* component as was done for the Sb/Ge case. At ~ 0.5 ML In coverage, essentially all Ge dimers are reacted, resulting in a BCN of ~ 2. However, to account for the intensity variation of the *C*

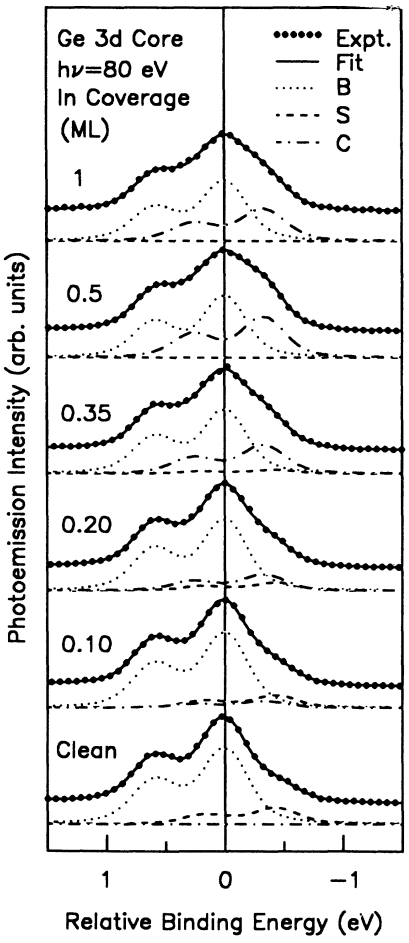

FIG. 9. The Ge 3*d* core-level spectra (dots) taken with a photon energy of 80 eV for clean Ge(100)-(2×1) and In-covered Ge(100). The coverages of In are indicated. The solid curves are the result of a fit to the data. The decomposition of the spectra into the bulk (*B*), surface (*S*), and interface (*C*) contributions are shown by the dotted, dashed, and dash-dotted curves, respectively. The relative binding energy scale is referred to the Ge $3d_{5/2}$ core-level component of the bulk contribution.

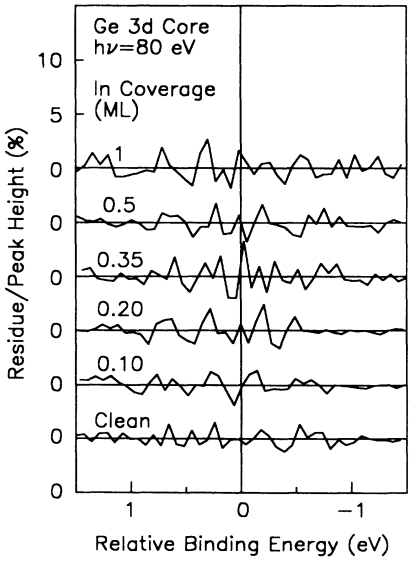

FIG. 10. The residue (difference between the data and fit) normalized to the peak height for those spectra shown in Fig. 9.

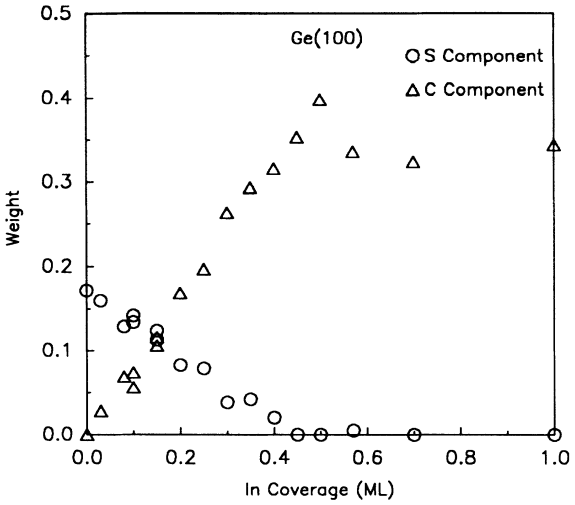

FIG. 11. The weight (fraction of total intensity) of the S (open circles) and (open triangles) components for various In coverages on Ge(100).

component as well, it is necessary to enhance the model. The discussion will be presented after the remaining data have been examined.

The position of the Fermi level relative to the band edges is shown in Fig. 12, and the data have been obtained by measuring the changes in the Ge bulk core-level binding energy relative to the Fermi level as for Sb/Ge(100) discussed earlier. The Fermi level is seen to gradually shift downward for increasing In coverages, and the final position is located approximately at the VBM. Thus, the Schottky-barrier height is roughly zero. This band-bending shift is opposite to the case for Sb/Ge(100), which showed the Fermi-level movement to-

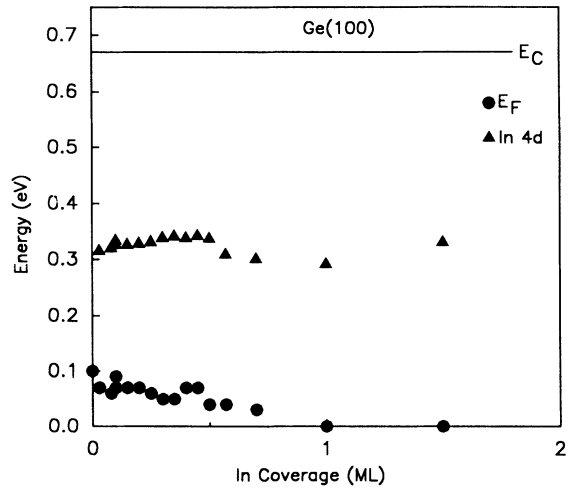

FIG. 12. The Fermi-level positions (solid circles) and the In $4d_{5/2}$ core-level binding energies (solid triangles) for various In coverages. The In $4d_{5/2}$ core-level binding energies have been offset 17.47 eV relative to the valence-band maximum (energy zero) to illustrate the correlations with the band edges. E_C denotes the conduction-band minimum of Ge.

wards the conduction-band minimum. This is to be expected qualitatively, since In is an acceptor and Sb is a donor in Ge.

C. In 4*d* core level

The In 4*d* core-level spectra are shown in Fig. 13. Like the Sb 4*d* core-level line shapes, the In 4*d* spectra were fitted with one spin-orbit split component. The Lorentzian width was constrained to equal 0.180 eV, which was the value obtained from the lowest coverage. The statistical average of the spin-orbit splitting and branching ratio for all coverages are 0.874 ± 0.008 eV and 0.709 ± 0.005, respectively. The In 4*d* Gaussian FWHM as a function of In coverage is shown in Fig. 14. The FWHM is relatively constant for coverages below 0.5 ML, suggesting that there is a good degree of uniformity for all of the bonding sites. At $\sim$0.5 ML there is a sudden increase; thus, additional sites with different binding energies are introduced resulting in the broadening. The In $4d_{5/2}$ binding energy relative to the VBM is shown in Fig. 12 alongside the Fermi-level data. The In $4d_{5/2}$ energy is offset 17.47 eV from its actual position to facilitate a comparison with the Fermi-level position and the band edges. The In 4*d* core position is seen to approximately remain constant, but a small sudden change of $\sim$0.03 eV is noted at $\sim$0.5 ML coverage. This is again correlated with the full development of the (2×2) phase.

D. Valence bands

The angle-integrated valence-band spectra for various In coverages taken with a photon energy of 80 eV are

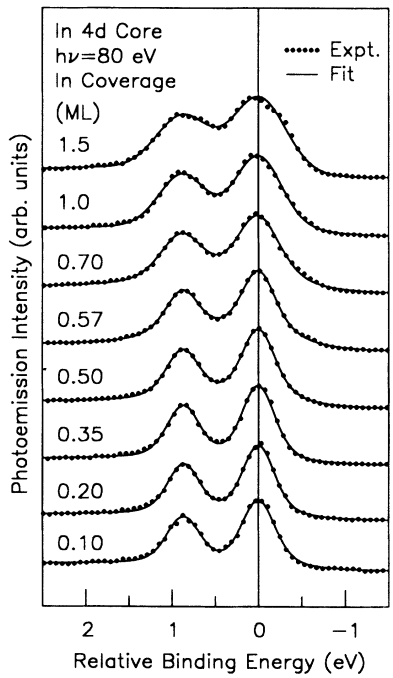

FIG. 13. The In 4*d* core-level spectra (dots) taken with a photon energy of 80 eV are shown for various In coverages. The lines represent the overall fit to the data. The binding energy is referred to the In $4d_{5/2}$ core-level component.

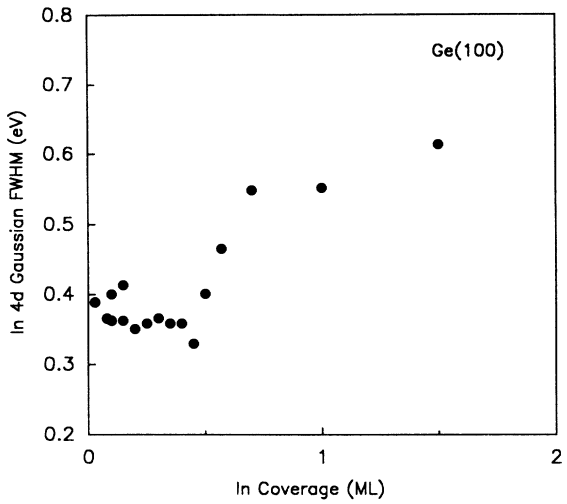

FIG. 14. The In 4*d* Gaussian FWHM for various In coverages on Ge(100).

shown in Fig. 15. The clean spectrum is shown at the bottom; the surface state at 1.2 eV binding energy is labeled *D*. The clean-surface spectra shown in Figs. 8 and 15 appear to be different, and this is due to the difference in photon energy used for each. The surface-state emission is reduced by In adsorption, in agreement with the interpretation that the surface dangling bonds are being saturated by In adatoms. However, due to the overlapping bulk emission, it is impossible to quantify the reduction. The behavior is similar to that observed for Sb/Ge(100) and In/Si(100).[1]

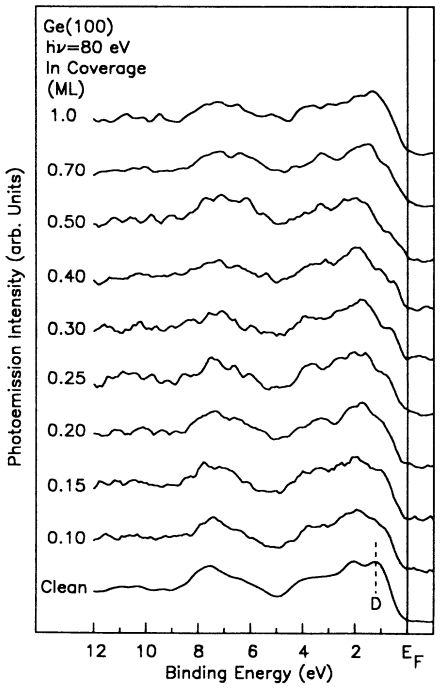

FIG. 15. Angle-integrated valence-band spectra taken with an 80 eV photon energy for various In coverages on Ge(100). The binding energy is referred to the Fermi level (E_F). The dashed line (labeled *D*) at 1.2 eV binding energy represents the position of the Ge dimer dangling-bond surface state.

V. DISCUSSION AND MODEL DEVELOPMENT

A. The In- and Sb-induced chemical shifts

Like the much studied Si(100)-(2×1) system, the principal mechanism leading to the surface shift of the Ge 3*d* core level is the increased electron localization about each dimer atom due to an unsaturated dangling orbital.[1,4–6,11] Upon adsorption, the dangling bonds rehybridize to form new chemisorption bonds. The binding-energy shift resulting from this bonding depends on the electronegativity of the adsorbate species. If the newly formed bond is covalent, then the surface Ge-atom binding energy will become bulklike, since its local bonding environment is bulklike. If, however, the bond is ionic, the charge transfer and the resulting shift in electrostatic potential will cause a chemical shift relative to the bulk atoms. From earlier studies of adsorption-induced shifts on Si(100) and Ge(100) surfaces, highly ionic chemisorption bonding is found to induce an energy shift of up to about 1 eV, and the shift is approximately proportional to the electronegativity difference.[11,22–25] The proportional factor has been empirically determined to be approximately 0.38 eV for unity difference in electronegativity based on the Sanderson scale.[11,24] We have chosen the Sanderson scale in this discussion instead of the Pauling scale, because the Sanderson scale was developed after the Pauling scale and represents an improvement.[24] There are, of course, other effects involved in the chemical shift, but the electronegativity model seems to account for the dominant part of the shift for all of the systems that have been examined so far.[11] The electronegativities of Ge, Si, In, Sb, As, and Ag are 3.59, 2.84, 2.84, 3.34, 4.11, and 2.57, respectively.[24] Therefore, for Sb adsorption on Ge(100) the conversion of the Ge 3*d* surface-atom emission to a component experimentally indistinguishable from the bulk emission is a consequence of the similarity in the electronegativities between Ge and Sb. The electronegativity model also suggests a chemical shift of about −0.29 eV relative to the bulk for In/Ge, which is very close to the value of −0.33 eV observed here.

B. Intensity of the chemically shifted core level

The adsorption of Ag on Ge(100) has been studied before.[17] A (1×1) HEED pattern was observed for coverages approaching 1 ML. The Ge 3*d* core-level line shape, however, remains unaltered as the weights and energy positions of the shifted component for the clean surface and the 1-ML-Ag-covered surface are the same. The observed chemical shift for Ag adsorption, same as the clean-surface shift, is again in good accord with the electronegativity model mentioned above. Note that the equivalence of the weight for the *S* component (the surface component for the clean surface) and *C* component (the chemically shifted component for 1-ML-Ag-covered surface) was originally believed to support the notion that the *S*-component emission is due to 1 ML of surface atoms.[17]

The most significant difference between In/Ge(100) and Ag/Ge(100) is the weight of the resulting *C* component relative to the *S* component, which is illustrated in Fig. 11 for In/Ge(100). A number of other photoemission studies have focused on the resulting intensity of the single interface core-level component for adsorbate-covered Ge(100) and Si(100) systems which show a partially ionic interface character and hence an observable chemical shift: As/Si(100),[26] Cl/Ge(100),[9] and S/Ge(100).[27] In each of these systems, the resulting intensity of the single interface component was greater than the intensity of the original surface component, but the increase depends on the adsorbate. Also in each case, the chemical shift is sufficiently large to be resolved easily, and the intensity increase of the surface component can be seen by visual inspection of the raw spectra without performing a fit (not the case for In/Ge). Previous counting of clean surface atoms has been performed by assuming that exactly 1 ML of adsorbates bond to 1 ML of surface atoms,[9,28] and the resulting intensity of the interface component was compared to the intensity of the surface-shifted component for the clean surface. Schnell *et al.* applied this procedure to Cl/Ge(100) and found that 0.62 ± 0.05 ML contribute to the clean-surface *S*-component emission.[9] This differs from the Ag/Ge(100) results and the 0.87 ± 0.09 ML obtained by the absolute determination technique.[10] Furthermore, the Ge(100)-(2×1) and Si(100)-(2×1) surfaces are expected to very similar, and an independent experiment based on a comparison between Si(100)-(2×1) and Si(111)-(7×7) found the *S*-component contribution to be 0.92 ± 0.07 ML for Si(100)-(2×1).[29] A recent theoretical calculation by Artacho and Ynduráin has also concluded that the *S*-component emission for the clean surface should be 1 ML (less the defects).[30]

Another relevent case is the As-saturated Si(100). This system is believed to form 1 ML of As dimers on the Si surface;[26] the main direct evidence comes from the STM results of Becker *et al.*[31] Bringans *et al.* showed that the As/Si(100) system exhibits an interface Si 2*p* core-level component which has a weight of 0.60 compared to the *S*-component weight of 0.17 for the clean surface.[26] A ratio of these two weights [as done with Cl/Ge(100) in Ref. 9] gives an *S*-component contribution of 0.28 ML; which is far below all of the values mentioned above.

The large discrepancies and variability in the *S*-component contributions determined by the adsorption-techniques discussed above are much beyond the typical variation in sample quality and suggest the need for model improvement. First, there is the possibility that the adlayer will unequally attenuate the interface layer which possesses reacted surface atoms and the subsurface layers which solely contribute to the bulk emission of the core level. This is easily visualized, for example, if the adsorbate bonding positions fall in sites located in the interface atomic plane so that only the subsurface emission is attenuated. But this effect is fairly small and cannot explain the large discrepancies noted above. Secondly, it is possible that chemisorption-bond formation may affect the core-level cross section of the reacted Ge atoms. There is some evidence for this effect. For example, Himpsel *et al.* have observed changes in the Si 2*p* photoionization cross section for the various oxidation states of oxygen adsorbed on Si.[32] The wave function of a core level is, of course, essentially decoupled from the environment. However, at the fairly low photon energies used in these core-level studies, the final states for core excitation are far from atomiclike, and therefore, a significant modification to the cross section due to a change in the chemical environment should be possible. Varma *et al.* have reported changes in the cross section of quasi-valence-band features of thin Hg films on Ag(100) which have been attributed to changes in environment.[33] There is not necessarily a direct, simple link between the change in cross section and the ionicity of the chemisorption bond;[32] structural effects could be much more important.[26] Indeed, the results for Cl, As, S, Sb, In, and Ag adsorption mentioned above do not show any obvious trend relating the ionicity of the chemisorption bond and the cross section change. Considering all of the above-mentioned results, a variation in the Ge 3*d* cross section caused by the In adsorption is the most likely explanation, and we will adopt this interpretation here. An inspection of the data in Fig. 11 shows that the cross-section enhancement is roughly a factor of 2.

C. Structural model for In/Ge(100)

The present photoemission and HEED results for In/Ge(100) are very similar to the results for In/Si(100).[1] For both systems, the HEED behavior shows a (2×2) pattern developing for In coverages approaching 0.5 ML, followed by another In-induced reconstruction. The In 4*d* Gaussian FWHM (Fig. 14) shows an approximately constant value for coverages below 0.5 ML, followed by a rapid increase. This suggests that all adsorption sites possess similar bonding configurations for coverages less than 0.5 ML, and new configurations are introduced for coverages greater than 0.5 ML.

Owing to the large correspondence between the In/Si(100) and In/Ge(100) systems, we propose that the same structural models proposed previously for In/Si(100) should also describe the behavior of In/Ge(100).[1] The models for low coverages (isolated adatoms) and 0.5 ML coverage [fully developed (2×2)] are shown in Figs. 16(a) and 16(b), respectively. The Ge(100) dimers are still present after In adsorption. At low coverages, each In adatom saturates three dangling bonds, because the chemical valence of In is 3. At 0.5 ML coverage, the In atoms form dimers with the dimer bond rotated 90° relative to the Ge dimer bonds. This (2×2) structure saturates all Ge dangling bonds and accounts for the valence of In. The In atoms probably lie close to the same plane as the Ge dimers to preserve the planar structure of the trivalent sp^2 configuration of In. For coverages greater than 0.5 ML, the In begins to fill sites other than those illustrated in Fig. 16(b), leading to the observed line broadening.

From the above structural models and assumed cross-section enhancement due to chemisorption, it is possible to use a discrete-layer attenuation model to analyze in detail the *S*- and *C*-component intensities shown in Fig. 11.

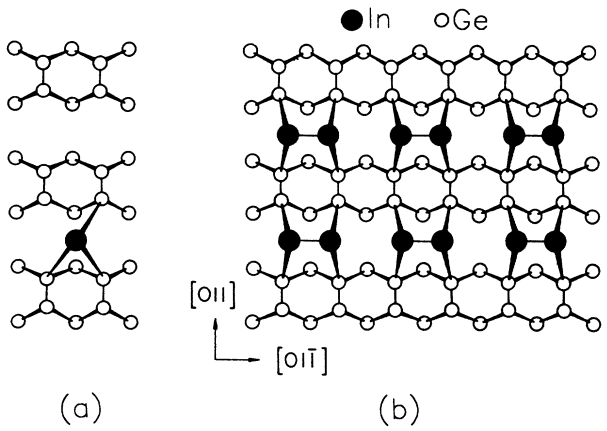

FIG. 16. A picture of structural models for (a) the adsorption position for an isolated In adatom on Ge(100) occurring at lower coverages, and (b) the ideal In/Ge(100)-(2×2) surface fully developed at 0.5 ML. The In and Ge atoms are illustrated by solid and open circles, respectively.

In the following analysis we assume a factor α, to be determined, for the enhanced cross section of the reacted dimer atoms relative to the unreacted dimer atoms. The intensities of the S, C, and B components of the Ge $3d$ core level (denoted I_S, I_C, and I_B, respectively) are given by the following equations:

$$I_S = X_S I_1 , \tag{1}$$

$$I_C = \alpha X_C I_1 , \tag{2}$$

$$I_B = \beta I_1 [(1-X_T) + e^{-d/l} + e^{-2d/l} + \cdots] , \tag{3}$$

and

$$\beta = 1 + 2(e^{-d/2l} - 1)\Theta , \tag{4}$$

where I_1 is the emission intensity for a Ge(100) monolayer, X_S and X_C are the fractions of a monolayer for the unreacted and reacted Ge dimer atoms, respectively, $X_T = X_S + X_C = 0.87$ ML is the total number of dimer atoms,[10] $d = 1.415$ Å is the interlayer spacing along the [100] direction, l is the phenomenological electron escape depth, β is an attenuation factor caused by the growth of In which affects only the subsurface emission, and Θ is the In coverage for coverages less than 0.5 ML. Equations (1)–(4) can be solved to yield

$$\alpha = \{X_T \beta^{-1} (I_B/I_C)[1 - X_T + (e^{d/l} - 1)^{-1}]^{-1} - I_S/I_C\}^{-1} , \tag{5}$$

$$X_S = \beta (I_S/I_B)[1 - X_T + (e^{d/l} - 1)^{-1}] , \tag{6}$$

and

$$X_C = \alpha^{-1} \beta (I_C/I_B)[1 - X_T + (e^{d/l} - 1)^{-1}] . \tag{7}$$

Using the experimental S-component weight for the clean surface, Eq. (6) gives $l = 6.4$ Å which agrees with previous results.[7,8] Equation (5) yields $\alpha = 2.3 \pm 0.3$ from a statistical average of the data in Fig. 11. Therefore, there is roughly a factor of 2 increase in the core-level cross section for the reacted Ge atoms. The In-to-Ge BCN is given by

$$n_{\text{BCN}}^{\text{In-to-Ge}} = (X_T - X_S)/\Theta = X_c/\Theta . \tag{8}$$

The BCN calculation from both the X_S and X_C values [Eqs. (6) and (7), respectively], using the average value for α, are shown in Fig. 17 using different symbols with a line showing the differences. The overall consistency is good. Although this is no proof that the model is correct, it shows that the assumed cross-section enhancement due to adsorption can explain all of the data. The BCN is seen to remain at ~2 for coverages below 0.5 ML. This corresponds very well with the model shown in Fig. 16(b) for the (2×2) structure. The BCN value should be 3 for the structure shown in Fig. 16(a) for the low-coverage limit. The interpretation here is that most of the In atoms form (2×2) islands already at the lowest coverage employed in this study; thus, the low-coverage limit is never realized in our experiment.

D. Structural analysis of Sb/Ge(100)

The Sb-to-Ge BCN values shown in Fig. 4 indicate a significantly different behavior than for In/Ge(100). The BCN is ~1 for coverages below 0.1 ML and increases to ~1.5 for coverages approaching 0.4 ML. For this type of behavior, together with the constancy of the (2×1) pattern observed in HEED for $T = 400$ °C, it is unlikely that the same sort of dimer pairing seen for In is the predominant bonding configuration for Sb. One possible structural model involves the replacement of Ge by Sb, similar to what has been reported before for the Sn/Si(100) system.[4] The models for low coverages (isolated adatoms) and ideal 1-ML-covered (2×1) surface are shown in Figs. 18(a) and 18(b), respectively. The electronic configuration for Sb in such a site is likely to be the

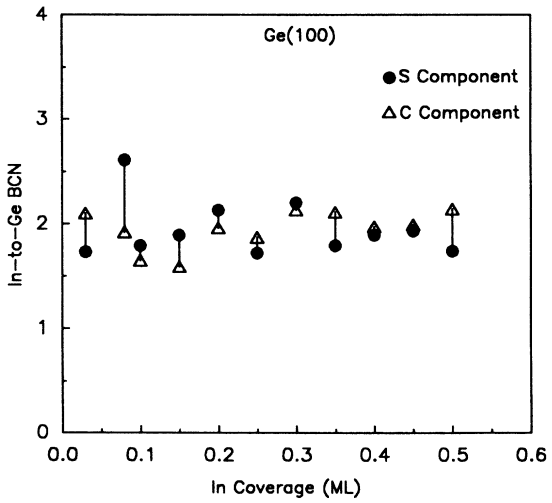

FIG. 17. The In-to-Ge BCN for various In coverages. The calculation using the S- and C-component weights are indicated by solid circles and triangles, respectively; a connecting line illustrates the differences.

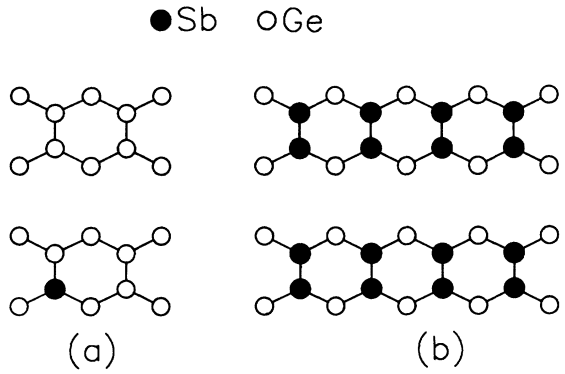

FIG. 18. A picture of structural models for (a) the adsorption position for an isolated Sb adatom on Ge(100) which represents a replacement site, and (b) the ideal 1 ML saturated Sb/Ge(100)-(2×1) surface. The Sb and Ge atoms are illustrated by solid and open circles, respectively.

trivalent s^2p^3 to account for the three bonds. The two s electrons form a nonbonding lone-pair orbital. The replacement site will have an effective BCN of 1, since each replacement Sb atom eliminates one Ge dangling bond. Because the BCN is ~1.5 for coverages approaching 0.4 ML, it is apparent that other bonding configurations must also exist for which one Sb atom modifies more than one Ge atom; the details of these configurations cannot be deduced from the present data but probably involve structures similar to the ones shown in Fig. 16. Because the atomic radius of Sb is significantly larger than that of Ge, the ideal (2×1) structure shown in Fig. 18(b) is probably not stable. The actual structure might involve defects and distortions to relieve the strain; this may explain the fact that the saturation coverage of Sb on Ge is somewhat less than 1 ML and the HEED pattern is somewhat diffuse at saturation coverage for $T=400$ °C. The correlation of the Sb 4*d* core-level binding energy with the VBM (Fig. 5) is also consistent with the replacement model.[4] The idealized structure shown in Fig. 18(b) happens to be the same structure proposed previously for As/Si(100)-(2×1) based on photoemission and STM results.[26,31]

For the related Sb/Si(100) system prepared at 350 °C, the BCN is initially 3 for low coverages and gradually approaches 2 for coverages approaching 0.5 ML,[6] which is different from that reported here for Sb/Ge(100). This indicates a fundamental difference between the interactions of Sb with Si(100) and Ge(100). For comparison, significant differences in behavior have also been reported before between Sb/Si(100) and As/Si(100).[6] Owing to the differences in atomic sizes, lattice constants, the electronegativities (reactivities), the various group-V and group-IV interface systems may or may not show similar behaviors.

VI. SUMMARY AND CONCLUSIONS

The initial stages of interface formation between In and Sb with the Ge(100) surface have been examined with photoemission and HEED. The adsorbate-induced core-level chemical shifts are seen to correlate with electronegativity differences. The photoemission intensities from the surface, interface, and bulk contributions of the Ge substrate core level are measured as a function of adsorbate coverage to yield the BCN. The present data and previously published data on other similar systems suggest that the core-level cross section may be significantly affected by a change in the local chemical environment of the atom. The degree of homogeneity of the adsorbate bonding is examined by measuring the widths of the adsorbate core levels. Photoemission from the valence bands shows the modification of the Ge dangling-bond surface states by the adsorbates. The variation of the Fermi-level position relative to the Ge band gap and the Schottky-barrier height are measured; the results are qualitatively consistent with the notion that In and Sb act as an acceptor and donor in Ge, respectively. Structural models are developed based on these results.

The present study applies the method of BCN determination as reported previously for a related substrate, Si(100). In principal, this technique should be applicable to any semiconductor surface which possesses a well defined surface atom core-level emission. For an improved understanding of III-V epitaxial growth, the study of fundamental interactions of group-III and -V atoms, each individually with group-IV semiconductor surfaces, is particularly essential. An optimization of the tailoring of interfaces and microstructures will require a detailed understanding of adsorbate behavior on the atomic level.

ACKNOWLEDGMENTS

This material is based upon work supported by the U.S. Department of Energy (Division of Materials Sciences of the Office of Basic Energy Sciences), under Contract No. DE-AC02-76ER01198. Some of the personnel and equipment support was also derived from grants from the National Science Foundation (Grants No. DMR-83-52083 and No. DMR-86-14234), the IBM Thomas J. Watson Research Center (Yorktown Heights, NY), and the E.I. du Pont de Nemours and Company (Wilmington, DE). We acknowledge the use of central facilities of the Materials Research Laboratory of the University of Illinois, which was supported by the U.S. Department of Energy (Division of Materials Sciences of the Office of Basic Energy Sciences), under Contract No. DE-AC02-76ER01198, and the National Science Foundation under Contract No. DMR-83-16981.

*Present address: Jet Propulsion Laboratory, California Institute of Technology, Pasadena, California 91109.

[1]D. H. Rich, A. Samsavar, T. Miller, H. F. Lin, T.-C. Chiang, J.-E. Sundgren, and J. E. Greene, Phys. Rev. Let. **58**, 579 (1987); D. H. Rich, A. Samsavar, T. Miller, H. F. Lin, and T.-C. Chiang, Mater. Res. Soc. Symp. Proc. **94**, 219 (1987).

[2]J. A. Kubby, J. E. Griffith, R. S. Becker, and J. S. Vickers, Phys. Rev. B **36**, 6079 (1987).

[3]R. J. Hamers, R. M. Tromp, and J. E. Demuth, Phys. Rev. B **34**, 5343 (1986).

[4]D. H. Rich, T. Miller, A. Samsavar, H. F. Lin, and T.-C. Chiang, Phys. Rev. B **37**, 10 221 (1988).

[5]A. Samsavar, T. Miller, and T.-C. Chiang, Phys. Rev. B **38**, 9889 (1988).

[6]D. H. Rich, F. M. Leibsle, A. Samsavar, E. S. Hirschorn, T. Miller, and T.-C. Chiang, Phys. Rev. B **39**, 12 758 (1989); D. H. Rich, T. Miller, G. E. Franklin, and T.-C. Chiang, *ibid.* **39**, 1438 (1989); D. H. Rich, G. E. Franklin, F. M. Leibsle, T. Miller, and T.-C. Chiang, *ibid.* **40**, 11 804 (1989).

[7]T. Miller, E. Rosenwinkel, and T.-C. Chiang, Solid State Commun. **47**, 935 (1983); **50**, 327 (1984).

[8]T. Miller, A. P. Shapiro, and T.-C. Chiang, Phys. Rev. B **31**, 7915 (1985).

[9]R. D. Schnell, F. J. Himpsel, A. Bogen, D. Rieger, and W. Steinmann, Phys. Rev. B **32**, 8052 (1985).

[10]D. H. Rich, T. Miller, and T.-C. Chiang, Phys. Rev. Lett. **60**, 357 (1988).

[11]See, for example, T.-C. Chiang, CRC Crit. Rev. Solid State Mater. Sci. **14**, 269 (1988); Mater. Res. Soc. Symp. Proc. **143**, 55 (1989).

[12]See, for example, Refs. 1 and 4–6; for Au and Ag on Si(111) and Ge(111), see, for example, A. L. Wachs, T. Miller, A. P. Shapiro, and T.-C. Chiang, Phys. Rev. B **35**, 5514 (1987).

[13]S. L. Hulbert, J. P. Stott, F. C. Brown, and N. Lien, Nucl. Instrum. Methods **208**, 43 (1983).

[14]R. A. Metzger and F. G. Allen, J. Appl. Phys. **55**, 931 (1984).

[15]S. A. Barnett, H. F. Winters, and J. E. Greene, Surf. Sci. **165**, 303 (1986).

[16]F. A. Trumbore, Bell Syst. Tech. J. **39**, 205 (1960); S. M. Hu, in *Atomic Diffusion in Semiconductors,* edited by D. Shaw (Plenum, New York, 1973), Chap. 5, p. 336.

[17]T. Miller, E. Rosenwinkel, and T.-C. Chiang, Phys. Rev. B **30**, 570 (1984).

[18]J. E. Rowe and S. B. Christman, J. Vac. Sci. Technol. **17**, 220 (1980).

[19]J. G. Nelson, W. J. Gignac, R. S. Williams, S. W. Robey, J. G. Tobin, and D. A. Shirley, Phys. Rev. B **27**, 3924 (1983); Surf. Sci. **131**, 290 (1983); P. Krüger, A. Mazur, J. Pollmann, and G. Wolfgarten, Phys. Rev. Lett. **57**, 1468 (1986).

[20]T. C. Hsieh, T. Miller, and T.-C. Chiang, Phys. Rev. B **30**, 7005 (1984).

[21]J. Knall, J.-E. Sundgren, G. V. Hansson, and J. E. Greene, Surf. Sci. **165**, 512 (1986).

[22]F. R. Mc Feely, J. F. Morar, N. D. Shinn, G. Landgren, and F. J. Himpsel, Phys. Rev. B **30**, 764 (1984).

[23]G. Hollinger and F. J. Himpsel, Phys. Rev. B **28**, 3651 (1983).

[24]R. T. Sanderson, *Chemical Bonds and Bond Energy* (Academic, New York, 1971).

[25]See also J. J. Joyce, M. Grioni, M. del Giudice, M. W. Ruckman, F. Boscherini, and J. H. Weaver, J. Vac. Sci. Technol. A **5**, 2019 (1987). These authors have examined the chemical shifts for GaAs.

[26]R. D. Bringans, M. A. Olmstead, R. I. G. Uhrberg, and R. Z. Bachrach, Phys. Rev. B **36**, 9569 (1987); **34**, 7447 (1986).

[27]T. Weser, A. Bogen, B. Konrad, R. D. Schnell, C. A. Schug, and W. Steinmann, Phys. Rev. B **35**, 8184 (1987).

[28]F. J. Himpsel, P. Heimann, T.-C. Chiang, and D. E. Eastman, Phys. Rev. Lett. **45**, 1112 (1980).

[29]D. H. Rich, T. Miller, and T.-C. Chiang, Phys. Rev. B **37**, 3124 (1988).

[30]E. Artacho and F. Ynduráin, Phys. Rev. Lett. **62**, 2491 (1989).

[31]R. S. Becker, J. S. Vickers, and T. Klitsner, Bull. Am. Phys. Soc. **33**, 785 (1988).

[32]F. J. Himpsel, F. R. McFeely, A. Taleb-Ibrahimi, and J. A. Yarmoff, Phys. Rev. B **38**, 6084 (1988).

[33]S. Varma, Y. J. Kime, P. A. Dowben, M. Onellion, and J. L. Erskine, Phys. Lett. **116**, 66 (1986).